Collective atomic effects in resonance fluorescence

G. S. Agarwal
Institute of Science, 15 Madame Cama Road, Bombay-400032, India

A. C. Brown
Physics Department, Brown University, Providence, Rhode Island 02912

L. M. Narducci
Physics Department, Drexel University, Philadelphia, Pennsylvania 19104

G. Vetri
Instituto di Fisica, Universita' di Palermo, Palermo, Italy
(Received 15 November 1976)

We suggest that the statistical properties of the scattered radiation in resonance-fluorescence experiments may be affected significantly by the existence of atomic correlations. The scattered light spectrum from two- and three-atom collective systems has been calculated and compared with the one-atom spectrum. The differences are quite significant for weak fields, but become less pronounced as the intensity of the driving field is increased. In addition, we have calculated the scattered intensity correlation function for collectively interacting systems, and found that its behavior is very different from that of the single-atom intensity correlation function, both for weak and strong incident fields. The implications of our findings for the observation of photon antibunching are also discussed.

I. INTRODUCTION

Resonance fluorescence, or the scattering of electromagnetic radiation by resonant atomic systems, is a familiar fundamental process,[1-4] that has become the focus of considerable attention in the last several years. In particular, the spectral distribution of the scattered light has been the subject of numerous theoretical[5-19] and experimental[20-24] investigations. At this time, it is well established that for incident field strengths below a certain threshold value, the scattered spectrum consists of a single broadened line, while, above threshold, it exhibits a pair of sidebands in addition to the central component. The ratio of the central line to the sideband peak-heights is 3:1, while the linewidth ratio is 1:1.5.

A new interesting feature of the scattered light has been discovered following a calculation of the second-order field-correlation function[25]:

$$G^{(2)}(t,t+\tau)=\langle E_s^{(-)}(t)E_s^{(-)}(t+\tau)E_s^{(+)}(t+\tau)E_s^{(+)}(t)\rangle\ , \tag{1.1}$$

where $E_s^{(+)}$ and $E_s^{(-)}$ are the positive- and negative-frequency parts of the scattered electric field operator, respectively.

It is well known that the second-order correlation function $G^{(2)}$ of the radiation emitted by a narrow-band thermal source has a maximum for $\tau\to 0$. This is, of course, a manifestation of the familiar photon-bunching effect which is characteristic of stationary thermal fields.[26] For increasing values of the delay τ, $G^{(2)}$ approaches the constant value

$$|G^{(1)}(0)|^2=|\langle E^{(-)}(t)E^{(+)}(t)\rangle|^2.$$

In the case of resonance fluorescence, instead, Carmichael and Walls have suggested that antibunching should occur for sufficiently small values of τ.

More precisely, their calculations show that at $\tau=0$, the second-order correlation function $G^{(2)}$ vanishes identically. For increasing values of τ, $G^{(2)}$ increases either monotonically, below threshold, or with oscillations, if the field amplitude is larger than the threshold value. The asymptotic value of $G^{(2)}$ for long delay times is $|G^{(1)}(0)|^2$ in both cases. The occurrence of photon antibunching has also been suggested in connection with subharmonic generation.[27] In the case of resonance fluorescence it appears that the observation of antibunching effects should be within reach of the available experimental techniques.

A common feature of all the theoretical treatments of resonance fluorescence is the assumption that each atom interacts with the source field independently of the other atoms in the surrounding space. Intuitively, this appears to be a good approximation especially for fields as intense as the ones that have been used experimentally to observe the spectrum of the scattered light under saturation conditions (i.e., well above threshold).

If the incident field is intense enough, and if the atomic density is sufficiently small, one expects the dynamical evolution of each atom to be governed primarily by its interaction with the applied field rather than with the reradiated field from all the other atoms.

We suggest, however, that the higher-order correlation properties of the scattered light may be affected significantly by atomic correlation, even under saturation conditions. For this reason we propose a model calculation to analyze the first- and second-order correlation functions of the scattered field when a number of atoms are undergoing correlated motion. Specifically, we study the spectral distribution of the scattered light from two- and three-atom systems in cooperative interaction. We also calculate the second-order correlation function for one- and two-atom systems for various incident field strengths.

Our results can be summarized as follows. Well below threshold, the spectrum of the scattered light from correlated atomic systems is significantly broader than that expected from the independent-atom model. For increasing field strength, and especially well above threshold, both collective and independent-atom systems produce identical spectra. Thus, well above threshold, we recover the typical central peak and sidebands even in the case of cooperative atomic motion. The peak-height ratio of the central line to the sidebands is still 3:1 in resonance, and the linewidth ratio is 1:1.5 as predicted by the various single-atom models.

The situation is quite different with regard to the second-order field correlation function. Here we have been forced to limit out numerical solutions to the two-atom case, but a reasonable extrapolation of the results indicates that, both below and above threshold, the second-order correlation function for cooperative systems differs significantly from the one calculated on the basis of the single-atom model. In particular, the antibunching effect is considerably reduced and is probably not observable if a sufficiently large number of atoms are interacting collectively.

In Sec. II, we discuss the model adopted in our calculation and outline the derivation of the steady-state spectrum and of the second-order correlation function. In Sec. III, we present the results of the numerical computations and discuss the main effects of the collective atomic motion on resonance fluorescence.

II. DESCRIPTION OF THE MODEL

We consider the collective motion of a small sample of two-level atoms under the influence of an external driving field in resonance with the atomic transition. The small-sample model has played a significant role in the early theoretical discussions of superradiance.[11] Here we consider the joint effect of the irreversible collective atomic decay in vacuum and of the pumping induced by the applied field. Since much of the preliminary mathematical development is reviewed in Ref. 11, we limit our considerations to the solution of the relevant equations of motion.

The atomic sample is an open system coupled to the second quantized radiation field. The initial state of the field is the product of a single-mode coherent state (the incident laser field) and of the vacuum state for the rest of the modes. We assume that the Rabi frequency of the applied field is much smaller than the atomic transition frequency.

A fully quantum electrodynamic calculation shows that the reduced density operator of the atomic system satisfies the master equation[11]

$$\frac{\partial \rho}{\partial t} = 2\gamma(S^- \rho S^+ - \tfrac{1}{2}\rho S^+ S^- - \tfrac{1}{2} S^+ S^- \rho) - ig[S^+ + S^-, \rho] - i\Omega[S^z, \rho], \quad \Omega = \omega_0 - \omega_f , \tag{2.1}$$

where $S^{\pm} = \sum_i S_i^{\pm}$ are the collective dipole operators, 2γ is the Einstein A coefficient for a single atom, and the coupling constant g equals $-\frac{1}{2}\vec{d}\cdot\vec{\mathcal{E}}_0^{(+)}$, with $\vec{\mathcal{E}}_0^{(+)}$ being the amplitude of the applied field. The frequency of the field is ω_f and the atomic transition frequency ω_0. The master equation (2.1) has been derived in the rotating-wave, Markoff, and Born approximations. Furthermore, the atomic density operator ρ evolves in a frame rotating with the angular frequency of the applied field.

Our objective is to calculate the atomic steady state correlation functions from the master equations (2.1) following the procedure outlined in Ref. (11). The link between the atomic polarization operators and the scattered field amplitude is provided by the relation[28]

$$\vec{E}^{(+)}(\vec{r}, t) = \vec{E}_0^{(+)}(\vec{r}, t) - \frac{\omega_0^2}{c^2 r}\,\hat{n}\times(\hat{n}\times\vec{d})S^-\left(t - \frac{r}{c}\right), \tag{2.2}$$

where $E^{(+)}$ is the positive frequency part of the total field operator, $E_0^{(+)}$ is the corresponding solution of the homogeneous wave equations, and $\hat{n}$ is the unit vector in the direction of observation.

Since the source-field operators and the atomic-polarization operators are directly proportional to one another, we limit our considerations to the atomic correlation functions

$$\Gamma^{(1)}(t+\tau, t) = \langle S^+(t+\tau) S^-(t)\rangle , \tag{2.3a}$$

$$\Gamma^{(2)}(t, t+\tau, t+\tau, t) = \langle S^+(t) S^+(t+\tau) S^-(t+\tau) S^-(t)\rangle . \tag{2.3b}$$

The scattered-field spectrum is proportional to the Fourier transform of Eq. (2.3a); the existence, or lack, of antibunching effects is predicted by Eq. (2.3b) for small values of the delay τ. Both $\Gamma^{(1)}$ and $\Gamma^{(2)}$ will be calculated under steady-state conditions, i.e.,, for $t \to \infty$.

For the case of a single two-level atom, analytic solutions for $\Gamma^{(1)}$ and $\Gamma^{(2)}$ can be obtained. When collective effects are important, instead, an analytic solution requires the diagonalization of 8×8 matrices (for the case of two two-level atoms) and 15×15 matrices (for the case of three two-level atoms). Hence, in what follows we first obtain the spectrum in a form, which can be easily adapted to numerical computations. We consider explicitly the procedure for two-atom systems and present numerical results. A similar calculation has been carried out also for the three-atom problem, but only the numerical solutions will be presented.

The starting point is the master equation (2.1) which we now project into the Hilbert space of the energy eigenstates $|j,m\rangle$ with $j=1$, and $m=0, \pm 1$. The matrix elements $\rho_{m,m'}(t)$ of the atomic-density operator satisfy the coupled equations

$$\frac{\partial}{\partial \tau}\rho_{m',m} = (\nu_{m'+1}\nu_{m+1})^{1/2}\rho_{m'+1,m+1} - \tfrac{1}{2}(\nu_m + \nu_{m'})\rho_{m',m} - i\beta(\nu_{m'}^{1/2}\rho_{m'-1,m} + \nu_{m'+1}^{1/2}\rho_{m'+1,m} - \nu_{m+1}^{1/2}\rho_{m',m+1} - \nu_m^{1/2}\rho_{m',m-1}), \tag{2.4}$$

where

$$\tau = 2\gamma t\,, \quad \beta = g/2\gamma\,,$$

and

$$\nu_1 = \nu_0 = 2, \quad \nu_{-1} = 0\,. \tag{2.5}$$

Upon identification of the eight independent-matrix elements of $\rho_{mm'}(t)$ with the components $\psi_i(t)$ of an eight-dimensional vector (see Appendix A), the set of coupled equations (2)–(4) can be cast into the matrix form

$$\frac{d\vec{\psi}}{dt} = L\vec{\psi} + \vec{I}, \tag{2.6}$$

where the inhomogeneous term $\vec{I}$ has only two nonzero components. (In the notation of Appendix A, we have $I_7 = -i\beta\sqrt{2}$, $I_8 = I_7^*$, $I_i = 0$ for $i \neq 7, 8$.) The Laplace transform of $\vec{\psi}(t)$ is given by

$$\hat{\vec{\psi}}(z) = M\vec{\psi}(0) + z^{-1}M\vec{I}, \quad M = (z-L)^{-1}\,, \tag{2.7}$$

where L is a nonsingular matrix with eight distinct eigenvalues. The steady-state density operator follows directly from Eq. (2.7),

$$\vec{\psi}(\infty) = \lim_{z\to 0} z\hat{\vec{\psi}}(z) = -L^{-1}\vec{I},$$

$$\psi_i(\infty) = i\beta\sqrt{2}\,(L_{i7}^{-1} - L_{i8}^{-1})\,. \tag{2.8}$$

The result (2.7) yields all the one time expectation values. The time evolution of $\psi_i(t)$ depends on the eigenvalues of the matrix $(z-L)$. For the case of a single atom, the eigenvalues are known to be

$$z_1 = -\tfrac{1}{2}\,, \quad z_{2,3} = -\tfrac{3}{4} \pm (\tfrac{1}{16} - 4\beta^2)^{1/2}\,. \tag{2.9}$$

The characteristic structure of the scattered spectrum above threshold ($\beta > \frac{1}{8}$) can be traced to the appearance of an imaginary part in $z_{2,3}$. For two- and three-atom systems, the eigenvalues of L appear to be distinct for all values of β used in our analysis. Still, in spite of the occurrence of additional pairs of complex-conjugate eigenvalues, the scattered spectra from two- and three-atom systems are characterized by only two sidebands symmetrically displaced around the central peak, for resonant fields stronger than the threshold value. The reason underlying this behavior of the scattered spectrum is discussed in Appendix B.

The atomic correlation function $\Gamma^{(1)}$ and $\Gamma^{(2)}$ can be calculated as a simple application of the regression theorem.[29-31] This theorem states that if M, Q, and N are members of a complete set of system operators $\{M_\mu\}$ and if the one-time averages can be expressed as

$$\langle M(t)\rangle = \sum_\mu O_\mu(t,t')\langle M_\mu(t')\rangle, \quad t > t'\,, \tag{2.10}$$

with $O_\mu(t,t')$ c-number functions of time, then two-time expectation values take the form

$$\langle Q(t')M(t)N(t')\rangle = \sum_\mu O_\mu(t,t')\langle Q(t')M_\mu(t')N(t')\rangle\,, \quad t > t'\,. \tag{2.11}$$

In particular, Q or N can be identified with the identity operator. The calculation of the first-order atomic correlation function requires knowledge of the one-time average of the polarization operators $S^\pm$

$$\langle S^+(t)\rangle = \mathrm{Tr}(\rho(t)S^+) = \sum_{m=-1}^{1}(\nu_{m+1})^{1/2}\rho_{m,m+1}(t) = \sqrt{2}\,(\psi_4(t) + \psi_6(t))\,, \tag{2.12}$$

$$\langle S^-(t)\rangle = \sqrt{2}\,(\psi_3(t) + \psi_7(t))\,. \tag{2.13}$$

Using Eq. (2.7), the Laplace transform of Eq. (2.12) takes the form

$$\langle \hat{S}^+(z)\rangle = \int_0^\infty e^{-zt}\langle S^+(t)\rangle\, dt$$

$$= \sqrt{2}\sum_{j=1}^{8}(M_{4j}+M_{8j})\psi_j(t_0)$$

$$+\sqrt{2}\,(i\beta\sqrt{2})\,z^{-1}(M_{48}-M_{47}+M_{88}-M_{87})\,. \quad (2.14)$$

To calculate the two-time correlation function we apply the regression theorem to (2.14). We illustrate the procedure for the $j=2$ term in (2.14). We first write $\psi_2(t_0)$ as the ensemble average of the appropriate system operator

$$\psi_2(t_0) = \rho_{0,0}(t_0)$$

$$= \langle 0|\rho(t_0)|0\rangle$$

$$= \mathrm{Tr}\,(\rho(t_0)|0\rangle\langle 0|)\,. \quad (2.15)$$

Now, in the application of the regression theorem, we need to know the expectation value

$$\mathrm{Tr}(\rho|0\rangle\langle 0|S^-) = \langle 0|S^-\rho|0\rangle$$

$$= \sqrt{2}\,\langle 1|\rho|0\rangle$$

$$= \sqrt{2}\,\psi_3\,. \quad (2.16)$$

Thus the $j=2$ term in (2.14) leads to

$$(M_{42}+M_{82})\psi_3(t_0)\,.$$

Using this procedure we finally find that the Laplace transform of the two-time correlation function, under steady-state conditions is

$$\hat{\Gamma}^{(1)}(z) = \int_0^\infty d\tau e^{-z\tau}\lim_{t\to\infty}\langle S^+(t+\tau)S^-(t)\rangle$$

$$= [2(M_{42}+M_{82})\psi_3(\infty)+2(M_{44}+M_{84})\psi_1(\infty)+2(M_{46}+M_{86})\psi_4(\infty)+2(M_{47}+M_{87})\psi_5(\infty)+2(M_{48}+M_{88})\psi_2(\infty)]$$

$$+2(\sqrt{2}\,i\beta)z^{-1}\{M_{48}-M_{47}+M_{88}-M_{87}\}(\psi_3(\infty)+\psi_7(\infty))$$

$$= A(z)+B(z)\,. \quad (2.17)$$

The Laplace transform has a contribution from the pole at $z=0$. This leads to the coherent part of the correlation function and should be subtracted from the total correlation function. The incoherent part is defined by

$$\hat{\Gamma}^{(1)}_{\mathrm{incoh.}}(z) = \hat{\Gamma}^{(1)}(z) - \frac{1}{z}\lim_{z\to 0} z\hat{\Gamma}^{(1)}(z)\,. \quad (2.18)$$

Hence, the incoherent part of the Laplace transform of the correlation function will be

$$\hat{\Gamma}^{(1)}_{\mathrm{incoh.}}(z) = A(z)+2(\sqrt{2}\,i\beta)(\psi_3(\infty)+\psi_7(\infty))$$

$$\times(\mathfrak{M}_{48}-\mathfrak{M}_{47}+\mathfrak{M}_{88}-\mathfrak{M}_{87})\,,$$

$$\mathfrak{M} \equiv L^{-1}(z-L)^{-1}\,, \quad (2.19)$$

where $\psi_j(\infty)$ $(j=1,2,\ldots,8)$ are given by Eq. (2.8). Since $\langle S^+(z)S^-\rangle$ is an analytic function of z for $\mathrm{Re}\,z \geq 0$ the spectrum of the scattered light is given by the real part of Eq. (2.19) after replacement of z with $i(\omega-\omega_f)$. Expression (2.19) should be compared with the incoherent part of the spectrum for a single two level atom given by

$$\hat{\Gamma}^{(1)}_{\mathrm{incoh.}}(z) = \frac{8\beta}{(\frac{1}{2}+4\beta^2)^2}\,\frac{z^2+2z+1+2\beta^2}{\det(z-L)}\,,$$

$$L = \begin{pmatrix} -1 & i\beta & -i\beta \\ 2i\beta & -\frac{1}{2} & 0 \\ -2i\beta & 0 & -\frac{1}{2} \end{pmatrix}. \quad (2.20)$$

The second-order atomic correlation function can be calculated as follows. First, we obtain the single-time average

$$\langle S^+(t)S^-(t)\rangle = \mathrm{Tr}[\rho(t)S^+S^-]$$

$$= 2[\psi_2(t)+\psi_1(t)]\,. \quad (2.21)$$

Next, we take the Laplace transform of Eq. (2.21) and substitute $\psi_i(z)$ with the solution given by Eq. (2.7). The result is

$$\langle S^+(z)S^-(z)\rangle = 2\sum_{j=1}^{8}(M_{2j}+M_{1j})\psi_j(t_0)$$

$$+2(\sqrt{2}\,i\beta)z^{-1}(M_{18}+M_{28}-M_{17}-M_{27})\,. \quad (2.22)$$

Finally, from the regression theorem, we obtain the Laplace transform of the steady-state correlation function

$$\hat{\Gamma}^{(2)}(z)=\int_0^\infty d\tau e^{-z\tau}\lim_{t\to\infty}\langle S^+(t)S^+(t+\tau)S^-(t+\tau)S^-(t)\rangle$$
$$=4\{(M_{22}+M_{12})\psi_1(\infty)+(M_{27}+M_{17})\psi_3(\infty)$$
$$+(M_{28}+M_{18})\psi_4(\infty)\}+4(\sqrt{2}\,i\beta)z^{-1}$$
$$\times\{M_{18}+M_{28}-M_{17}-M_{27}\}(\psi_2(\infty)+\psi_1(\infty)), \tag{2.23}$$

where $\psi_j(\infty)$ is given again by Eq. (2.7).

As already observed,[32] the Laplace transform of the second-order correlation function $\Gamma^{(2)}(\tau)$ can be cast into the form

$$\Gamma^{(2)}(z)=\frac{A}{z}+g(z), \tag{2.24}$$

where A is a constant and $g(z)$ is a regular function of z for $\mathrm{Re}z\geq 0$.

More explicitly, in the single-atom case one has

$$\hat{\Gamma}^{(2)}(z)=(i\beta)^2z^{-1}(L_{12}^{-1}-L_{13}^{-1})(M_{13}-M_{12}), \tag{2.25}$$

which, when inverted, leads to

$$\Gamma^{(2)}(\tau)=1-\exp(-\tfrac{3}{4}\tau)[(3/4\Delta)\sin\Delta\tau+\cos\Delta\tau],$$
$$\Delta=(4\beta^2-\tfrac{1}{16})^{1/2}. \tag{2.26}$$

As shown in Ref. 25, Eq. (2.26) predicts antibunching for sufficiently short values of the delay τ [see Figs. 8–12, curve (a)]. The term A/z is responsible for the coherent (time independent) part of the second-order correlation.

It is clear from Eq. (2.23) that, in the limit $t\to\infty$, the steady-state (s.s.) correlation function becomes

$$\lim_{t\to\infty}\langle S^+S^+(t)S^-(t)S^-\rangle_{\mathrm{s.s.}}=\lim_{z\to 0}z\langle S^+S^+(z)S^-(z)S^-\rangle_{\mathrm{s.s.}}$$
$$=4(i\beta\sqrt{2})(L_{17}^{-1}+L_{27}^{-1}-L_{18}^{-1}-L_{28}^{-1})$$
$$\times[\psi_1(\infty)+\psi_2(\infty)], \tag{2.27}$$

which, by using Eq. (2.7), reduces to

$$\lim_{t\to\infty}\langle S^+S^+(t)S^-S^-\rangle_{\mathrm{s.s.}}=4[\psi_1(\infty)+\psi_2(\infty)]^2$$
$$=\langle S^+S^-\rangle_{\mathrm{s.s.}}^2. \tag{2.28}$$

Hence, in our numerical analysis we refer to the normalized correlation function

$$\gamma^{(2)}(t)=\frac{\langle S^+S^+(t)S^-(t)S^-\rangle_{\mathrm{s.s.}}}{\langle S^+S^-\rangle_{\mathrm{s.s.}}^2},\quad \gamma^{(2)}(\infty)=1. \tag{2.29}$$

The inverse Laplace transform of Eq. (2.23) offers technical problems. It cannot be performed analytically because of the large size of the matrix L. In addition, a direct numerical integration appears to be unfeasible due to the enormous number of time-consuming matrix inversions that are required for every value of z. We found it expedient to apply the theorem of residues. Thus, the matrix elements $(z-L)^{-1}_{m,n}$ and $(L^{-1}(z-1)^{-1})_{m,n}$ have been calculated as the ratio of the appropriate cofactors and determinants. The typical contribution of the pole z_i of the integrand reduces to

$$\underset{z_i}{\mathrm{Residue}}\,[e^{z\tau}(z-L)^{-1}_{m,n}]=e^{z_i\tau}\,\frac{\mathrm{Cofactor}(z_i-L)_{nm}}{\prod_{j\neq i}(z_i-z_j)}. \tag{2.30}$$

This process has worked well for two atoms, but, unfortunately, has not produced useful results for the three-atom case due to the large numerical values taken up by the cofactors and the subsequent loss of numerical accuracy.

The results of the calculation and the comparison with the analytic solutions for the single-atom model are given in Sec. III.

III. FIRST- AND SECOND-ORDER CORRELATION FUNCTIONS OF THE SCATTERED LIGHT

The linear relation between the scattered-field operators and the atomic-source operators [Eq. (2.2)] implies that the atom and field correlation functions are directly proportional to one another. We analyze first the numerical results of the steady-state spectrum of the incoherent scattered light. For convenience, the spectra have been normalized to unity at $\omega=\omega_0$ and the results of the one-, two- and three-atom systems have been superimposed in the figures. In the single-atom case the (3×3) matrix L has three distinct eigenvalues, two of them complex conjugates of one another, above threshold. Thus, it is natural to trace the origin of the three spectral components to the poles of Eq. (2.20).

For two- and three-atom systems the situation is more complicated. The corresponding L matrices are (8×8) and (15×15), respectively. Our analysis of the eigenvalues of L for different values of the pump field strength reveals that they are distinct and that their imaginary parts can be considerably different from one another. Still the structure of the scattered spectrum displays no additional peaks. In fact, well above threshold, the shape of the scattered spectrum for two- and three-atom systems approaches the one predicted by the single-atom model. This behavior can be understood in terms of selection rules which are operative for radiative transitions between different energy levels of the collective atom-pump field states. In the limiting case of intense incident pump fields, the selection rules are derived and discussed in Appendix B.

The results of our numerical calculations are shown in Figs. 1–5 where half of the spectra are plotted for different values of the resonant field

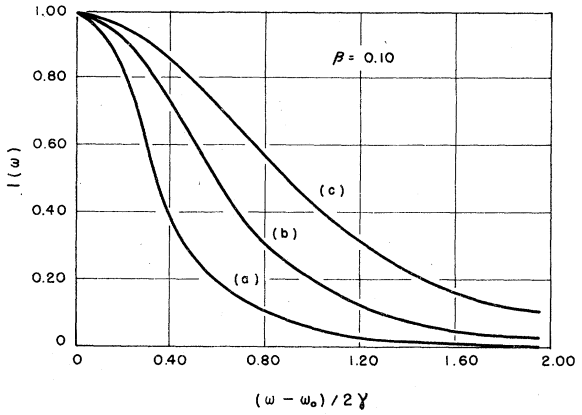

FIG. 1. Steady-state spectra of the incoherent scattered light from (a) one atom, (b) two atoms, (c) three atoms. The spectra are symmetric around $(\omega-\omega_0)/2\gamma = 0$. The applied field amplitude is proportional to β. The value $\beta = 0.1$ corresponds to a field amplitude below threshold for single-atom resonance fluorescence.

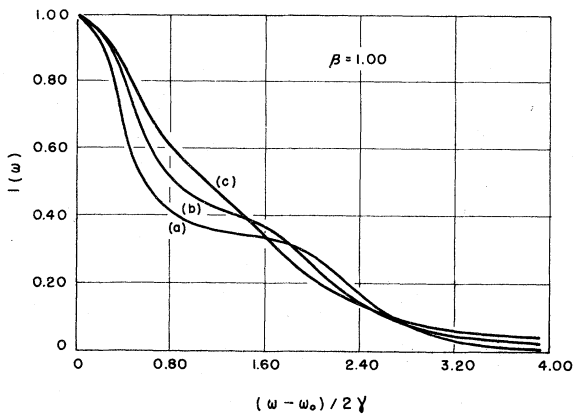

FIG. 3. Same as Fig. 1 but with larger applied field ($\beta = 1.00$).

strength (the spectra are symmetric around the central frequency $\omega = \omega_0$, as we have verified). According to these results, the effect of correlated atomic motion is especially pronounced for weak applied field. The deviations from the predicted single-atom spectra may not be easily observed because of unavoidable experimental uncertainties with the absolute values of the measured linewidth. In addition, in our calculation we have ignored the effects of the so-called first-order dispersion forces[33] which, sometimes, may be important.

It appears, instead, that intensity correlation measurements of the scattered light should provide a more definitive test of the existence of collective effects. As already discussed in Refs. 25 and 19, a striking property of the scattered light is the predicted photon antibunching which is expected for short delay times. Roughly speaking, the existence of antibunching stems from the fact that, after the first emission process, the atom requires a finite amount of time before being excited again. If a larger number of atoms are interacting collectively with the pump field, the above qualitative argument does not apply. In fact, for intense pump fields, the steady-state density operator approaches the limiting form

$$\rho(\infty) = \frac{1}{2j+1} \sum_{m=-j}^{j} |jm\rangle\langle jm| , \tag{3.1}$$

where j is the usual cooperation number, and $|j,m\rangle$ are the eigenstates of the collective atomic energy operator S_z. For small values of the delay time τ, the normalized second-order correlation function $\gamma^{(2)}(\tau)$ [Eq. (2.29)] is different from zero.

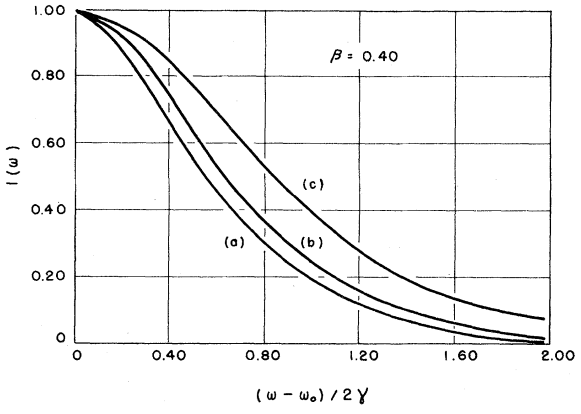

FIG. 2. Same as Fig. 1 but with larger applied field ($\beta = 0.40$).

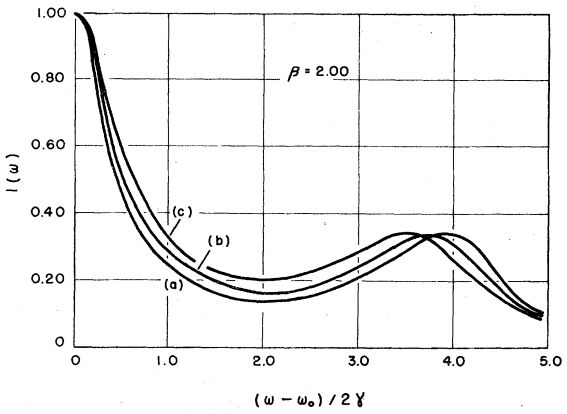

FIG. 4. Same as Fig. 1 but with larger applied field ($\beta = 2.00$).

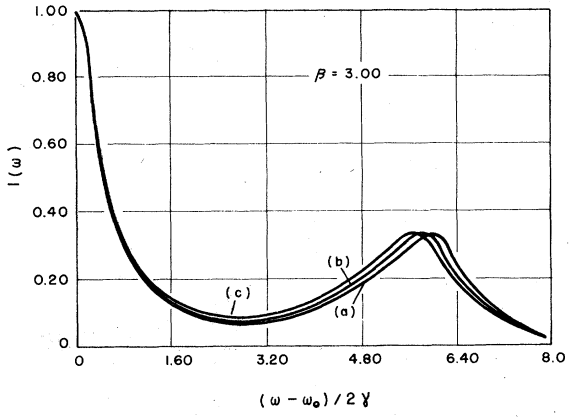

FIG. 5. Same as Fig. 1 but with applied field strength well above threshold ($\beta = 3.00$).

In fact, at $\tau = 0$ and in the strong-field limit, $\gamma^{(2)}$ equals 0.75 for two atoms, 0.96 for three, and becomes slightly greater than unity for a large number of atoms (note that the $\tau \to \infty$ limit of $\gamma^{(2)}$ is unity by definition). Thus it appears that collective effects should reduce the antibunching drastically.

The strong-field limit of $\rho(\infty)$ given by Eq. (3.1) can be obtained from Eq. (2.14) if one expands the steady-state solution in powers of β^{-1}. To zeroth order in β^{-1}, one finds $\rho_{m,m} = \rho_{m-1,m-1}$ for all m, if

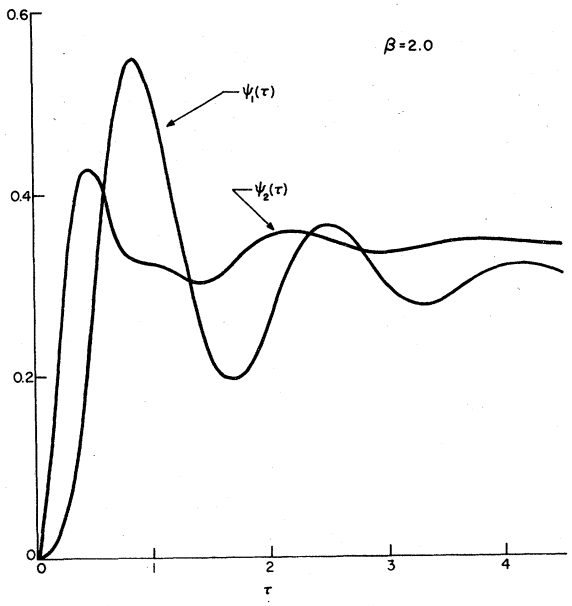

FIG. 6. Time dependence of the diagonal density matrix elements $\psi_1(\tau) = \rho_{11}(\tau)$ and $\psi_2(\tau) = \rho_{0,0}(\tau)$ for the two-atom system. The time axis is measured in units of $(2\gamma)^{-1}$ [Eq. (2.4)].

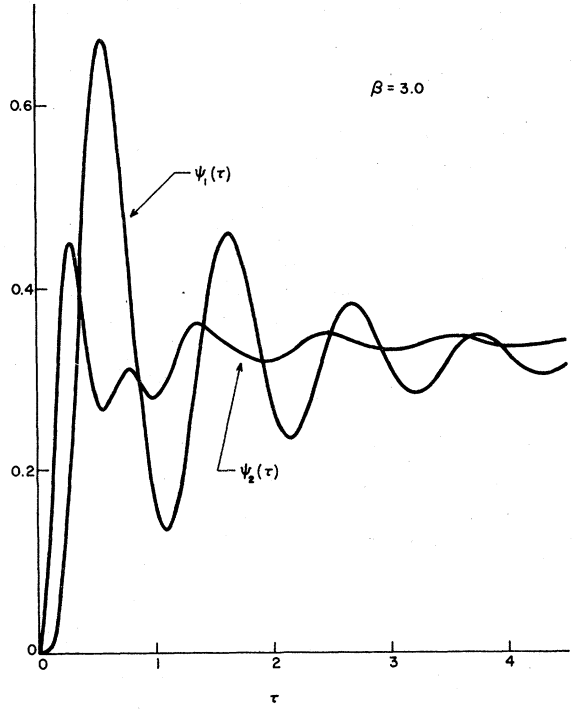

FIG. 7. Time dependence of the diagonal density matrix elements $\psi_1(\tau) = \rho_{1,1}(\tau)$ and $\psi_2(\tau) = \rho_{0,0}(\tau)$ for the two-atom system. The field amplitude corresponding to $\beta = 3$ is well above threshold. The long-time limit of ψ_1 and ψ_2 is very close to $\frac{1}{3}$. The time axis is measured in units of $(2\gamma)^{-1}$ [Eq. (2.4)].

the off-diagonal elements are zero to the same order of approximation. The off-diagonal matrix elements of $\rho(\infty)$ can be shown to be zero for the single-atom case. For the two-atom problem, the above is supported by our numerical calculations as shown in Figs. 6 and 7 and Table I.

A complete antibunching effect will be found again in the case of the two-atom resonance fluorescence if we examine the higher-order correlation function

$$\Gamma^{(3)} = \langle S^+(t)S^+(t+\tau_1)S^+(t+\tau_1+\tau_2) \times S^-(t+\tau_1+\tau_2)S^-(t+\tau_1)S^-(t)\rangle . \quad (3.2)$$

TABLE I. Steady-state values of the density-matrix elements for the two-atom case.

τ	β	$\mathrm{Im}\psi_3$	$\mathrm{Re}\psi_5$	$\mathrm{Im}\psi_7$
10	2	−0.1083	−0.0383	−0.1219
	5	−0.0463	−0.0065	−0.0473
	10	−0.0233	−0.0016	−0.0234
	15	−0.0088	−0.0003	−0.0155

$\mathrm{Re}\psi_3 = \mathrm{Im}\psi_5 = \mathrm{Re}\psi_7 = 0$, $\psi_4 = \psi_3^*$, $\psi_6 = \psi_5^*$, $\psi_8 = \psi_7^*$.

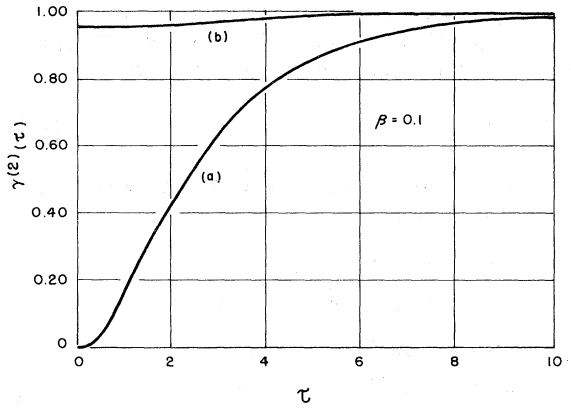

FIG. 8. The normalized atomic correlation functions $\gamma^{(2)}(\tau)$, [Eq. (2.29)], for (a) one and (b) two-atom systems plotted as functions of the dimensionless time τ.

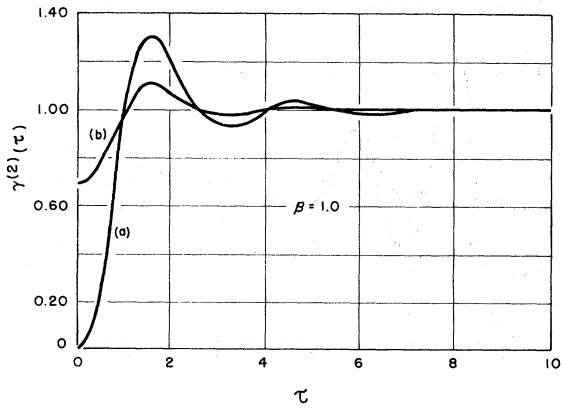

FIG. 10. Same as Fig. 8 but with larger applied field ($\beta = 1.00$).

This correlation function, which is proportional to the probability of detecting three photons, one at time t, a second at $t+\tau_1$, and the third at $t+\tau_1+\tau_2$, vanishes for $\tau_1=\tau_2=0$ and thus shows a complete antibunching effect. The mathematical reason for such a result is the operator relation $(S^+)^3=(S^-)^3=0$ for a system of two two-level atoms. The physical reason is that, in order for the detector to detect three photons, the time scales should be such that the atoms have a chance to be raised into one of the excited states by the interaction with the laser field.

The normalized second-order correlation function $\gamma^{(2)}(\tau)$ for the collective two-atom system is shown in Figs. 8–12 for different values of the pump field strength. For comparison the one-atom second-order correlation function is also shown. We observe that the oscillations of $\gamma^{(2)}(\tau)$ are characteristic of the oscillations of the diagonal matrix elements $\rho_{m,m}(\tau)$ as we can see, for example, upon inspection of Figs. 12 and 7. The reason for this behavior is that, when the applied field is strong, then, to lowest order in the incoherent interaction, the atomic system will be found approximately in an "atomic coherent state," if it was in the ground state at the beginning.[34,35] The amplitude of the atomic coherent state is $|z| = |\tan(gt)|$. Since the atomic expectation values are functionals of $|z|$, they will tend to exhibit the same periodic behavior as $|z|$ itself, independently of the number of atoms.

In summary, our results indicate that correlated atomic motion should cause a significant broadening of the steady-state spectrum below threshold, but should have little observable effect well above threshold. Thus careful observations of the spectrum below threshold should provide another evidence of the superradiant effects. Such observations would, of course, be free from the

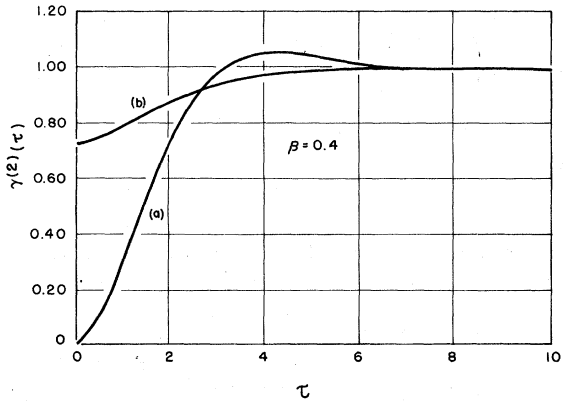

FIG. 9. Same as Fig. 8 but with larger applied field ($\beta = 0.40$).

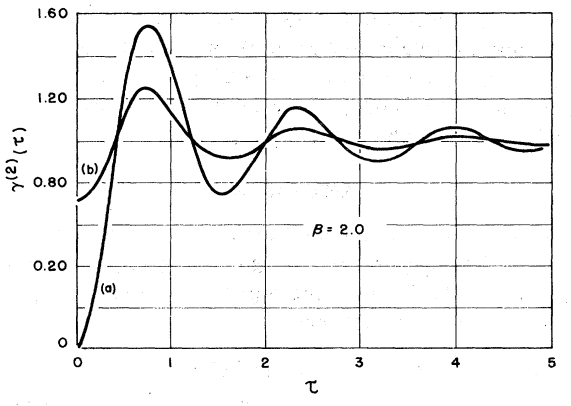

FIG. 11. Same as Fig. 8 but with larger applied field ($\beta = 2.00$).

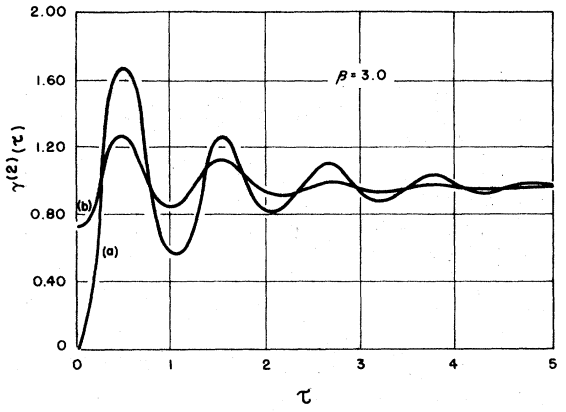

FIG. 12. Same as Fig. 8 but with applied field strength well above threshold ($\beta = 3.00$).

usual complications arising due to geometrical effects and propagation effects. In addition, the second-order correlation function shows that the scattered radiation from collectively interacting systems has quite a different statistical character from the field scattered by uncorrelated atoms. We find that correlated motion tends to eliminate antibunching for weak fields and to reduce it considerably for more intense pump strength.

Note added in proof. After submission of the manuscript an important contribution by Bonifacio and Lugiato was brought to our attention. In the context of their analysis of optical bistability these authors [Opt. Commun. (to be published)] have clarified several aspects of the steady-state behavior of resonance fluorescence from a collection of two-level systems.

ACKNOWLEDGMENTS

Two of us (G.S.A. and G.V.) carried out the work reported in this paper while visiting the Worcester Polytechnic Institute. They would like to thank the Quantum Optics Group for its hospitality during the course of the visit. P. C. Colby's assistance with some of the numerical work is gratefully acknowledged.

APPENDIX A

We consider the coupled differential equations (2.4) for the matrix elements of the atomic density operator. We identify the eight components $\psi_i(t)$ of the vector ψ as follows:

$$\begin{aligned} &\rho_{1,1}=\psi_1, \quad \rho_{0,0}=\psi_2, \quad \rho_{-1,-1}=\psi_9=1-\psi_1-\psi_2, \\ &\rho_{1,0}=\psi_3, \quad \rho_{0,1}=\psi_4, \quad \rho_{1,-1}=\psi_5, \\ &\rho_{-1,1}=\psi_6, \quad \rho_{0,-1}=\psi_7, \quad \rho_{-1,0}=\psi_8. \end{aligned} \tag{A1}$$

While the correspondence (A1) is entirely arbitrary, the calculations developed in Sec. II depend on it. Thus we find that the vector equation

$$\frac{d\vec{\psi}}{dt}=L\vec{\psi}+\vec{I} \tag{A2}$$

is a compact representation of the following eight coupled equations:

$$\begin{aligned} \dot{\psi}_1 &= -2\psi_1 - i\beta\sqrt{2}(\psi_4-\psi_3), \\ \dot{\psi}_2 &= 2\psi_1 - 2\psi_2 - i\beta\sqrt{2}(\psi_8+\psi_3-\psi_4-\psi_7), \\ \dot{\psi}_3 &= -2\psi_3 - i\beta\sqrt{2}(\psi_2-\psi_1-\psi_5), \\ \dot{\psi}_4 &= -2\psi_4 - i\beta\sqrt{2}(\psi_6+\psi_1-\psi_2), \\ \dot{\psi}_5 &= -\psi_5 - i\beta\sqrt{2}(\psi_7-\psi_3), \\ \dot{\psi}_6 &= -\psi_6 - i\beta\sqrt{2}(\psi_4-\psi_8), \\ \dot{\psi}_7 &= 2\psi_3 - \psi_7 - i\beta\sqrt{2}(\psi_5-\psi_1-2\psi_2) - i\beta\sqrt{2}, \\ \dot{\psi}_8 &= 2\psi_4 - \psi_8 - i\beta\sqrt{2}(2\psi_2-\psi_6+\psi_1) + i\beta\sqrt{2}. \end{aligned} \tag{A3}$$

The inhomogeneous term of Eq. (A2) is a vector $\vec{I}$ with components

$$I_7=-i\beta\sqrt{2}, \quad I_8=i\beta\sqrt{2}, \quad I_i=0, \quad i\neq 7,8. \tag{A4}$$

Note added in proof. On introducing the variables

$$\begin{aligned} &\Phi_1=\psi_3-\psi_4, \quad \Phi_2=\psi_7-\psi_8, \quad \Phi_3=\psi_5+\psi_6, \\ &\chi_1=\psi_3+\psi_4, \quad \chi_2=\psi_7+\psi_8, \quad \chi_3=\psi_5-\psi_6, \end{aligned} \tag{A5}$$

we find that Eqs. (A3) can be divided into two independent sets, i.e.,

$$\begin{aligned} \dot{\psi}_1 &= -2\psi_1 + g'\Phi_1, \\ \dot{\psi}_2 &= 2\psi_1 - 2\psi_2 - g'(\Phi_1-\Phi_2), \\ \dot{\Phi}_1 &= -2\Phi_1 - g'(2\psi_2-2\psi_1-\Phi_3), \\ \dot{\Phi}_2 &= 2\Phi_1 - \Phi_2 - g'(\Phi_3-4\psi_2-2\psi_1) - 2g', \\ \dot{\Phi}_3 &= -\Phi_3 - g'(\Phi_2-\Phi_1) \end{aligned} \tag{A6}$$

and

$$\begin{aligned} \dot{\chi}_1 &= -2\chi_1 + g'\chi_3, \\ \dot{\chi}_2 &= 2\chi_1 - \chi_2 - g'\chi_3, \\ \dot{\chi}_3 &= -\chi_3 - g'(\chi_2-\chi_1), \end{aligned} \tag{A7}$$

where

$$g'=i\beta\sqrt{2}.$$

It is easy to show that the steady-state solution of these equations is unique and is

$$\begin{aligned} &\chi_1=\chi_2=\chi_3=0, \\ &\Phi_1=\frac{2g'^3}{D}, \quad \Phi_2=-\frac{2g'(1-g'^2)}{D}, \quad \Phi_3=\frac{2g'^2}{D}, \\ &\psi_1=\frac{g'^4}{D}, \quad \psi_2=-\frac{g'^2(1-g'^2)}{D}, \end{aligned} \tag{A8}$$

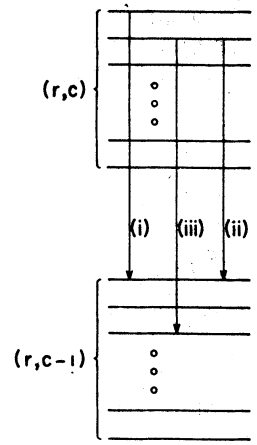

FIG. 13. Schematic energy-level diagram showing typical downward spontaneous transitions for a multiatom system initially prepared in one of the states of the (r,c) multiplet. Transition (i) occurs with the emission of a quantum of energy equal to the atomic transition energy. Transition (ii) is responsible for the appearance of the downshifted sideband of the spectrum. Transition (iii) contributes to the upshifted sideband of the spectrum. The energy levels in both multiplet are nearly equispaced for large values of c (incident field strength well above threshold).

where

$$D = 3g'^4 - 2g'^2 + 1, \quad D \neq 0 .$$

It is clear from Eq. (A8) that in the limit of strong field, $g' \gg 1$, the only nonvanishing components of $\vec{\psi}$ are

$$\psi_1 = \psi_2 = \tfrac{1}{3}, \quad g' \gg 1 . \tag{A9}$$

Equation (A9) confirms explicitly our relation (3.1). The time dependent solution of Eqs. (A7) is straightforward, however the system of equations (A6) presents technical difficulties because of problems in solving a fifth-degree polynomial equation. For our numerical work, we have chosen to use the original set (A3).

APPENDIX B

The mathematical origin of the three peaks in the spectrum of resonance fluorescence from a single atom has been traced in the main text to the three distinct eigenvalues of the (3×3) matrix L.

Above threshold, one eigenvalue of L is real, while the others are complex conjugate of one another. The imaginary parts of the eigenvalues determine the location of the center of the spectral components, while the real parts give a measure of their width. It would be incorrect to generalize this argument to the case of resonance fluorescence from collective atomic systems.

The purpose of this appendix is to show that, due to selection rules which become operative for multiatom systems, the spontaneous radiative decay of N two-level systems in resonant interaction with an applied field also gives rise to a three-peak spectrum. The sidebands are symmetrically displaced around the applied driving frequency by the same amount predicted in the case of single-atom resonance fluorescence. Our considerations are valid in the case of strong applied fields and explain some of the quantitative features of the numerical results displayed in Fig. 5. ($\beta = 3$ corresponds to a sufficiently intense applied field so that our perturbative argument can be safely applied).

We consider the exact eigenstates of a coupled system comprised of N atoms and a resonant single mode of the applied field. Furthermore, we assume the atomic system to be prepared in a collective state of cooperation number r. If we neglect counterrotating terms the Hamiltonian of the system is

$$H = a^\dagger a + S_z + K(a^\dagger S^- + a S^+) , \tag{B1}$$

where K is the atom-field coupling constant. Its eigenstates can be classified into multiplets labeled by the indices r (the atomic cooperation number) and c ($c = n + m$ where n is the field excitation number and m is the eigenvalue of S_z). Both r and c are good quantum numbers in the absence of symmetry breaking mechanisms. If the applied field is sufficiently intense ($c \gg r$), it has been shown in Ref. 36 that the eigenstates of the Hamiltonian (B1) have the structure.

$$|r,c,m\rangle = \sum_{m'=-r}^{r} d^{(r)}_{m,m'}\left(\frac{\pi}{2}\right) |r,m'\rangle\,|c-m'\rangle , \tag{B2}$$

where $d^{(r)}_{mm'}(\frac{1}{2}\pi)$ are the matrix elements of the rotation operator $\exp[i(\frac{1}{2}\pi)S_y]$ in the representation in which S_z is diagonal.[37] The states $|r,m'\rangle$ and $|c-m'\rangle$ are the eigenstates of S^2 and S_z and of $a^\dagger a$, respectively. The index m of the eigenstates takes on $2r+1$ integral on half-integral values with $|m| \leq r$. The energy corresponding to the mth eigenstate of the (r,c) multiplet is

$$E_m = c + 2K\sqrt{c}\,m, \quad |m| \leq r . \tag{B3}$$

A system described by the Hamiltonian (B1) is now coupled to the vacuum of radiation. We are interested in evaluating the transition amplitude for spontaneous emission of one photon into an arbitrary mode of the vacuum. While this perturbative argument cannot provide information on the details of the emitted spectrum, it will provide us with the appropriate selection rules for the spontaneous radiative transition.

With the added symmetry breaking contribution

of the atom-vacuum interaction, c is no longer a good quantum number. The cooperation number r is assumed, instead, to be conserved during the collective decay of the atomic system. Thus, the required transition amplitude between the initial state $|\text{vac}\rangle\,|r,c,m_1\rangle$ and the final state $|0,\ldots,1\ldots0\ldots\rangle\,|r,c',m_2\rangle$ is proportional to the matrix element

$$\langle r,c',m_2|S^-|r,c,m_1\rangle=\delta_{c',c-1}\sum_{m_3=-r}^{r} d^{(r)}_{m_1,m_3}\left(\frac{\pi}{2}\right)d^{(r)}_{m_2,m_3-1}\left(\frac{\pi}{2}\right)[(r+m_3)\,(r-m_3+1)]^{1/2}. \tag{B4}$$

The sum on the right-hand side of Eq. (B4) can be easily carried out if we observe that

$$\begin{aligned}\sum_{m_3=-r}^{r} d^{(r)}_{m_1,m_3}\left(\frac{\pi}{2}\right)d^{(r)}_{m_2,m_3-1}\left(\frac{\pi}{2}\right)[(r+m_3)\,(r-m_3+1)]^{1/2} &= \langle r,m_2\,|\,e^{i\pi/2S_y}S^-e^{-i\pi/2S_y}|r,m_1\rangle\\ &= m_1\delta_{m_1,m_2}-\tfrac{1}{2}[(r-m_1)\,(r+m_1+1)]^{1/2}\delta_{m_2,m_1+1}\\ &\quad-\tfrac{1}{2}[(r+m_1)\,(r-m_1+1)]^{1/2}\delta_{m_2,m_1-1}.\end{aligned} \tag{B5}$$

Equation (B5) provides the required selection rules. With the help of Fig. 13 the physical situation can be understood as follows: The multiplets (r,c) and $(r,c-1)$ are radiatively coupled to one another. For $c\gg r$, the energy levels of each multiplet are equally spaced by an amount $2K\sqrt{c}$. The only possible transitions correspond to (i) $m_2=m_1(m_1\neq0)$ with the emission of a quantum of energy equal to the single-atom level spacing, (ii) $m_2=m_1+1$ with the emission of a quantum of energy $1-2K\sqrt{c}$ (in units of atomic transition energy), (iii) $m_2=m_1-1$ with the emission of a quantum of energy $1+2K\sqrt{c}$. All other transitions are forbidden. These results are independent of the cooperation number.

[1]V. Weisskopf and E. Wigner; Z. Phys. 63, 54 (1930); 65, 18 (1931).
[2]V. Weisskopf, Ann. Phys. Leipz. 9, 23 (1931).
[3]V. Weisskopf, Z. Phys. 85, 451 (1933).
[4]W. Heitler, *Quantum Theory of Radiation*, 3rd Ed. (Oxford U. P., London), p. 36, p. 196–203.
[5]M. C. Newstein, Phys. Rev. 167, 89 (1968).
[6]B. R. Mollow, Phys. Rev. 188, 1969 (1969); Phys. Rev. A 5, 1522 (1972).
[7]C. R. Stroud, Phys. Rev. A 3, 1044 (1971).
[8]C. R. Stroud, *Coherence and Quantum Optics*, edited by L. Mandel and E. Wolf (Plenum, New York, 1973), p. 537.
[9]C. S. Chang and P. Stehle, Phys. Rev. A 4, 641 (1971).
[10]R. Gush and H. P. Gush, Phys. Rev. A 6, 129 (1972).
[11]G. S. Agarwal, in Springer Tracts Mod. Phys. 70, 1 (1974). The rate of change of photons in some mode ks was calculated as

$$\begin{aligned}\sigma_{ks}(t)&=\dot{N}_{ks}(t)\\ &=\langle a^\dagger_{ks}(t)\dot{a}_{ks}(t)\rangle\\ &=|g_{ks}|^2\int_0^t d\tau e^{-i\omega_{ks}(t-\tau)}\langle S^+(t)S^-(\tau)\rangle+\text{c.c.}\\ &=|g_{ks}|^2\int_0^t d\tau e^{-i\omega_{ks}\tau}\langle S^+(t)S^-(t-\tau)\rangle+\text{c.c.},\end{aligned}$$

and thus in the steady state

$$\begin{aligned}\sigma_{ks}(\infty)&=|g_{ks}|^2\int_0^\infty d\tau\, e^{-i\omega_{ks}\tau}\lim_{t\to\infty}\langle S^+(t)S^-(t-\tau)\rangle+\text{c.c.}\\ &=|g_{ks}|^2\int_0^\infty d\tau\, e^{-i\omega_{ks}\tau}\langle S^+(\tau)S^-(0)\rangle_{\text{s.s.}}+\text{c.c.}\\ &=|g_{ks}|^2\int_{-\infty}^\infty d\tau\, e^{-i\omega_{ks}\tau}\langle S^+(\tau)S^-(0)\rangle_{\text{s.s.}}.\end{aligned}$$

Hence it is clear that the rate of change of photons in the mode ks is proportional to Mollow's spectrum. As a matter of fact one can show that Eq. (18.19) of Ref. 11 coincides with the incoherent part of Mollow's spectrum [Eq. (18) of Ref. 6] if the transformation $\alpha\to\Omega/2,\gamma\to k/2$ to Mollow's notation is made. Of course, in the derivation of Eq. (18.19) of Ref. 11 the coherent part was ignored.
[12]S. S. Hassan and R. K. Bullough, J. Phys. B 8, L147 (1975).
[13]B. R. Mollow, Phys. Rev. A 12, 1919 (1975).
[14]B. R. Mollow, J. Phys. A 8, L11 (1975).
[15]H. J. Carmichael and D. F. Walls, J. Phys. B 8, L77 (1975).
[16]S. Swain, J. Phys. B 8, L437 (1975).
[17]C. Cohen-Tannoudji, in *Frontiers in Laser Spectroscopy*, *XXVII Les Houches Summer School*, edited by R. Balcan, S. Haroche, and S. Liberman (North-Holland, Amsterdam, 1976).
[18]H. J. Kimble and L. Mandel, Phys. Rev. Lett. 34, 1485 (1975).

[19]H. J. Kimble and L. Mandel, Phys. Rev. A 13, 2123 (1976).
[20]F. Schuda, C. R. Stroud, and M. Hercher, J. Phys. B 7, L198 (1974).
[21]W. Hartig and H. Walther, Appl. Phys. 1, 171 (1973).
[22]W. Lange, J. Luther, B. Nottbeck, and H. W. Schroder, Opt. Commun. 8, 157 (1973).
[23]H. Walther, *Proceedings of the Second Laser Spectroscopy Conference*, edited by S. Haroche *et al.* (Springer-Verlag, Berlin, 1975), p. 358.
[24]F. Y. Wu, R. E. Grove, and S. Ezekiel, Phys. Rev. Lett. 35, 1429 (1975).
[25]H. J. Carmichael and D. F. Walls, J. Phys. B 9, L43 (1975).
[26]R. Hanbury-Brown and R. W. Twiss, Nature 177, 27 (1956); 178, 1046 (1956).
[27]D. Stoler, Phys. Rev. Lett. 33, 1397 (1974).
[28]G. S. Agarwal, Phys. Rev. A 12, 1475 (1975), Eq. (6.8); see also Ref. 11, Eq. (7.13); and J. H. Eberly and N. Rehler, Phys. Rev. A 3, 1735 (1971).
[29]M. Lax, Phys. Rev. 172, 350 (1968).
[30]H. Haken and W. Weidlich, Z. Phys. 205, 96 (1967).
[31]M. Lax, in *Statistical Physics, Phase Transitions and Superfluidity*, edited by M. Chretien, E. P. Gross, and S. Deser (Gordon and Breach, New York, 1968), Vol. 2, p. 269.
[32]In a recent paper [G. S. Agarwal, Phys. Rev. A 15, 814 (1977)] it has been shown that the correlation function $\langle S^{+}S^{+}(z)S^{-}(z)S^{-}\rangle$ associated with a two-level atom undergoing Markovian dynamics has always the structure (2.24).
[33]M. J. Stephen, J. Chem. Phys. 40, 669 (1964). See also the discussion by Agarwal in Ref. 11, Chap. 6 and additional references therein.
[34]F. T. Arecchi, E. Courtens, and R. Gilmore, H. Thomas, Phys. Rev. A 6, 2211 (1972).
[35]J. Kutzner, Z. Phys. 259, 177 (1973).
[36]L. M. Narducci, M. Orszag, and R. A. Tuft, Phys. Rev. A 8, 1892 (1973).
[37]A. R. Edmonds, *Angular Momentum in Quantum Mechanics* (Princeton U. P., Princeton, N. J., 1957).